FACHHOCHSCHULE **TRIER**
Hochschule für Technik, Wirtschaft und Gestaltung
University of Applied Sciences
Informatik

Informatik-Bericht Nr. 2008-9

Schriftenreihe Fachbereich Informatik, Fachhochschule Trier

MER Classification for Deep Brain Stimulation

Peter Gemmar, Oliver Gronz, Thorsten Henrichs,
Frank Hertel[†], Christian Decker[‡]
Institute for Innovative Informatics-Applications i3A,
University of Applied Sciences (FH) Trier, Germany*
[†] Hospital Idar-Oberstein, Germany
[‡] Hospital of the Merciful Brethren, Trier, Germany

Preprint: Sixth Heidelberg Innovation Forum, April 15, 2008

Abstract

Deep brain stimulation (DBS) of the subthalamic nucleus (STN) has become a common procedure to alleviate the symptoms of advanced Parkinson's disease. To estimate the optimal site for placement of the definite electrode, up to five microelectrodes are inserted at first and the neuronal activity at the electrode tip is recorded. These microelectrode recordings (MER) are classified to STN or non-STN signals manually by the surgeon, which requires experience and time.

A system has been developed for automatic classification of MER signals. The classifier consists of three levels, each of which using a specific criterion to decide whether a MER is STN signal or not. In the first level, the background activity is examined and those recordings showing increased activity are marked. The second level uses the bursty or irregular behavior of typical STN single cell activity for taking decisions. In the last level, the spike rate of duplicated intervals resulting from level 1 and 2 is examined. Results from all levels are combined and thus STN signals are identified.

To enhance the evaluation of the different characteristics, signal preprocessing is performed in level 2 and level 3. Wavelet transformation is used to remove background activity (noise) and a multilevel 1-d wavelet decomposition is used to extract certain properties of the signals.

The classifier has been tested using 2434 MERs taken from 14 patients. Nearly 95% of the classifications matched with a specialist's decision. The remaining differences were mainly due to signals lacking distinctive characteristics, especially signals extracted near the border of STN.

The classifier will support the surgeon and make the decision process for the final electrode position more reliable and less time consuming. It can easily be adapted for the classification of other functional neural areas than the STN.

Keywords: DBS, STN, MER, signal classification, wavelet transformation, Parkinson's disease

1 Introduction

Stereotactic deep brain stimulation is a widespread treatment option for different kinds of neurological diseases, especially movement disorders, such as Parkinson´s disease (PD), Dystonia, different kinds of tremors, or chronic pain also ([1],[2]). In the treatment of advanced PD the STN is considered the most promising target. In this procedure, electrodes are implanted permanently in the patient's STNs. They emit signals that reduce the effect of the chronic hyperactivity of STN. Especially for long-term patients,

*Contact: Prof. Dr. Peter Gemmar, Fachhochschule Trier, Schneidershof, 54293 Trier, Germany; p.gemmar@fh-trier.de

who suffer from side effects of the medical treatment or who experience strong fluctuations in results of medical treatment, this procedure is actually the most promising therapy.

In the planning phase of the procedure, the target point is identified using different image modalities like T1 and T2 weighted magnetic resonance images (MRIs). Due to deviations between the image based targeting and the position eventually reached (e.g. [3] or [4]), up to five microelectrodes are inserted at first, to determine the optimal site for the definite electrode. The local and extra cellular electrical activity at the tip of each microelectrode is measured and visualized during surgery. These MERs are classified as STN or non-STN signals by the surgeon.

As a result of MER classification – either manually or automatically – the sections of each electrode's trajectory are labeled, which pass through the STN. The neurosurgeon can use this information to create a geometric association of the labeled sections with the anatomic shape of the STN by imagination. Now, having the seeming positions of the electrodes in mind, the neurosurgeon can estimate the real target location and finally determine the position of the stimulating electrode.

Classification of the MERs is sometimes ambiguous even for experienced neurosurgeons. There are different approaches for automatic analysis and classification of MER signals using statistical features or digital spike trains [5, 6, 7]. In the following we introduce a method for MER classification based on soft-denoising and multi-level decomposition of the MER signals. The method extracts features for a multi-level geometric classifier independent from specific patient characteristics.

The classifier supports the surgeon to a great extend. It generalizes the procedure for positioning the final electrode and makes it more reliable and less time consuming.

2 Materials and Methods

MERs presented in the following were recorded using microelectrodes, microdrive and Leadpoint^{TM}from Medtronic Inc. They were recorded at the Hospital of the Merciful Brethren in Trier, Germany. The sampling rate of all MERs is $24kHz$, the signal length is $10s$.

Accordingly, all interval sizes or other thresholds described were determined with respect to these conditions. The complete procedure can be adapted easily to handle higher sampling rates or longer sequences. For the usage of lower sampling rates or shorter sequences, further testing procedures are mandatory.

2.1 STN Signal Properties

Within the last decade, the main characteristics of STN signals and useful methods to identify them have been examined and described thoroughly (e.g. [8] and [9]). Accordantly, the most useful criteria for recognition of STN signals are the distribution of spikes and bursts and an increased background noise (see Figs. 1 and 2).

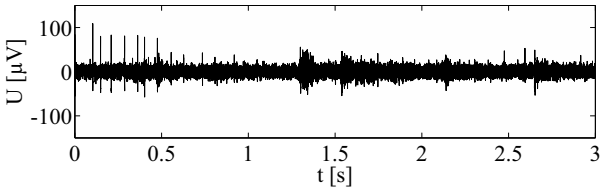

Figure 1: MER of an area without neuronal activity

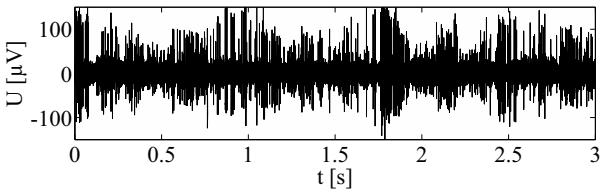

Figure 2: MER in the proximity of STN neurons

In different publications, the main characteristics for the discrimination of the signals are described similarly. Nevertheless, the quantitative data about the most important features - spike rate and spike distribution - differ in various papers, which seams to be natural, as these values differ from person to person.

A typical trajectory might intersect the overlying zona incerta before the electrode reaches STN and finally the underlying substantia nigra (SNr). As up to five electrodes are used, at least two or three of them will show STN signals. Benazzouz et. al. [8] describe the signals vividly: "During a typical exploratory track, we can observe a very low background noise in the zona incerta and almost complete absence of single cell recording. Penetration of the electrode tip into the STN is characterized by a sudden increase in background activity and single cell activity of spontaneously active neurons. The exit of electrode tip out of the STN corresponds to a decrease in background noise and a loss of single cell activity. Spontaneous neuronal activity increases again when the electrode tips enter the substantia nigra pars reticulata (SNr)".

In addition, the pattern of single cell activity in the SNr is a more regular tonic activity while STN cells exhibit an irregular or bursty firing pattern. Hutchinson [9] describes a mean firing rate inside STN of $37 \pm 17 spikes/s$, for SNr $71 \pm 23 spikes/s$. Benazzouz [8] measured $42.3 \pm 22 spikes/s$ for STN. Obviously, there is no universally valid threshold to distinguish between STN and SNr. For some patients, the firing rate of SNr might be lower than STN's firing rate of other patients or vice versa. Additional information that can support the classification besides the characteristics already mentioned is the length of an individual trajectory displaying typical STN activity.

2.2 Classifier's Architecture

Based on this knowledge about characteristical criteria of the concerned neural structures, the classifier consists of three levels. Each of these levels decides whether a specific criterion is fullfilled or not. At first, MERs from potential areas with neural activity are marked. In the second step, those marked areas are inspected with respect to the irregular bursting pattern of STN. A key element of this step is the usage of wavelets to de-noise signals and to analyze only specific frequency ranges. In some cases, multiple intervals along the electrode path are classified as STN signals according to the second level. Those intervals are then handled by the third step that examines the spike distribution.

The complete procedure works without global thresholds concerning spike distribution or firing rate. All MERs of one electrode are inspected together and patient-specific thresholds are determined automatically where it is necessary.

2.3 Level 1: Finding Neuronal Sections

In the following, a single MER is represented by a vector s. The length of this vector is $samplingrate[Hz] \cdot windowsize[s]$. For one electrode, n recordings are available, thus each signal $s_i, 1 \leq i \leq n$ represents the recording in one depth and $s_{i,j}$ describes the j-th discrete sample of recording i.

In this level, the MERs of potential neuronal activity are marked in the set of MERs of one electrode. Therefore, the background activity is used as the decisive criterion. To judge whether background activity is stronger or not, two different thresholds are determined and used. The first threshold t_{med} is calculated by

$$t_{med} = \frac{\sum_{i=1}^{n} median(|s_i|)}{n} \cdot c \qquad (1)$$

where $median(|s_i|)$ is the median of absolute values of MER s_i, which is the 50th percentile of the absolute values of signal s_i. Additionally, the mean standard deviation of all MERs is calculated by:

$$t_{std} = \frac{\sum_{i=1}^{n} \sigma_i}{n} \cdot c \quad . \qquad (2)$$

Scaling the thresholds by factor c is necessary for those electrodes that do not show any STN signals. For them, both median and standard deviation of different recordings s_i will approximately be the same for all $i, 1 \leq i \leq n$. Thus, some signals will exceed the threshold although they show no neuronal activity. Real STN signals will exceed the threshold plainly, so the threshold is increased. The value of factor c has been determined using test data and seems to be optimal.

In the next step, each s_i is subdivided into l_1 intervals with a length of $||s_i||_2/l_1[s]$. For each interval of each signal $s_i, 1 \leq i \leq n$, the standard deviation and the median of absolute values is calculated.

Now we can simply count the intervals that exceeded t_{med} and thus calculate the ratio of this number to the total number of intervals of one recording. This result is stored in a vector of length n, where each element represents the ratio of one signal s_i. Accordingly, the same is done for those intervals that exceed t_{std}. Finally, the two vectors are combined by calculating the mean element by element.

For the following, let I be the set of indices of signals s_i that were identified as neuronal active according to the first level. These are the signals, the ratio of which exceeded a given percentage p. Unfortunately, all $i \in I$ are not necessarily connected: several subsets of recordings can belong to I where other recordings $s_j, j \notin I$ were measured in between.

2.4 Signal Preprocessing for Level 2 and 3

Intensified background activity has been used as the decisive criterion in the first level. The following two levels concentrate on spikes, their number and their distribution. To handle the spikes in an optimal manner, the background activity should be removed as well as possible, which is described in the following section. Afterwards, the signal can be processed easier and we will concentrate on certain components of this signal using multilevel 1-d wavelet decomposition. This transformation results in a set of coefficients which is the actual input of level 2 and 3.

2.4.1 De-Noising by Soft-Thresholding

At first, we analyze the background activity in more detail in order to removing it optimally. We can assume that two different sources are responsible for the background activity. The first source is the activity of a large set of neurons in different distances to the electrode. The second source might be noise produced by the recording system itself, which is present for signals outside STN, too.

Concentrating on the first source, the signal s_i and each sample $s_{i,j}$ respectively is a sum of:

- strong single cell activity of spontanesously active neurons close to the electrode, which produces the so-called spikes, and
- activity of a large set of neurons firing independently and in random manner.

Thus, the samples $s_{i,j}, 1 \leq i \leq n, 1 \leq j \leq m$ can be approximated as a sum of single cell activity $\widehat{s}_{i,j}$ and independent and identically distributed standard Gaussian random variables z_j:

$$s_{i,j} = \widehat{s}_{i,j} + z_j, i = 1, \ldots, n, j = 1, \ldots, m \quad . \tag{3}$$

The noise produced by the recording system can be described equally. Thus, it is contained here too.

To remove this kind of noise or to estimate the unknown signal $\widehat{s}_i$ "De-noising by Soft-Thresholding" [10] is an effective tool. The result $\widetilde{s}_i$ of this estimator fullfills two different criteria. Firstly, with high probability $\widetilde{s}_i$ is at least as smooth as $\widehat{s}_i$ in any of a wide variety of smoothness measures and secondly, the estimator comes nearly as close in mean square to $\widehat{s}_i$ as any measurable estimator can come to (according to [10]). The principle of this method is illustrated in Fig. 3.

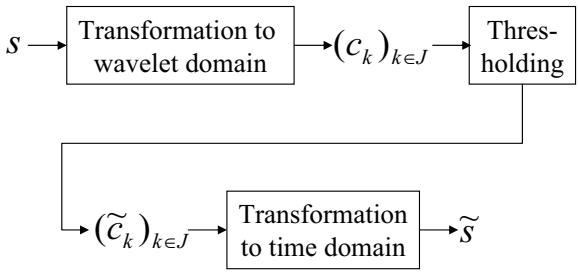

Figure 3: Principle of denoising by thresholding in wavelet domain

The measured signal s_i represents the neuronal activity at the electrode in time domain. This signal is transformed to wavelet domain resulting in a set of coefficients $(c_k)_{k\in J}$. A threshold τ is determined and the set is transformed using this threshold. Finally, the modified coefficients $(\widetilde{c}_k)_{k\in J}$ are transformed back to time domain, resulting in the estimation $\widetilde{s}_i$.

Wavelet transformation [11] is one way to describe a signal s as a linear combination

$$s = \sum_{k\in J} c_k \psi_k. \tag{4}$$

Where $(\psi_k)_{k\in J}$ is a set of orthonormal basis functions and J is a finite set of indices. Unlike Fourier transformation, information about the point in time when certain frequencies appear in time domain is preserved by wavelet transformation.

Good estimations of unknown signals $\widehat{s}_i$ can be achieved under the following circumstances [12]:

- True signal $\widehat{s}_i$ should be from a class of signals that can be approximated well by few coefficients using $(\psi_k)_{k\in J}$.
- Noise should be of a kind that cannot be compressed using $(\psi_k)_{k\in J}$. (White noise, which is the kind of noise we want to remove, cannot be compressed at all using orthonormal bases.)
- Level of noise is small compared to the unknown signal.

The last interesting aspect concerning our excursion on de-noising is the modification of coefficients (for additional information on estimation of τ, see e.g. [10] or [12]). Unlike in hard-thresholding, the coefficients falling below τ are not just simply set to zero; modification of coefficients is done by shrinking them:

$$\widetilde{c}_k := \begin{cases} 0 & if|c_k| \leq \tau \\ sign(c_k)(|c_k| - \tau) & if|c_k| > \tau \end{cases} . \quad (5)$$

Fig. 4 shows the result of the process. The background activity contained in the original signal (Figure 2) is nearly completely removed and only the spikes remain.

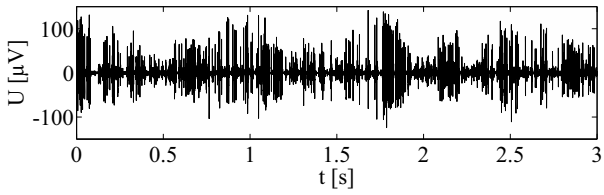

Figure 4: Signal shown in Fig. 2 after noise reduction

2.4.2 Multilevel 1-D Wavelet Decomposition

Multilevel 1-D wavelet decomposition (wavedec) can be compared to a microscope: $\widetilde{s}_i$ can be viewed with any desired scaling (magnification) at any point in time. Therefore, wavedec uses a scaling function ϕ, where ϕ is a short, majoritarian positive impulse [12].

In each level of the process, the signal is split into two parts (see Fig. 5). One part is convolved with a high-pass ϕ_{high} followed by dyadic decimation (downsampling) resulting in the detail coefficients cD_1 of level 1. The other part is convolved with a low-pass ϕ_{low} followed by dyadic decimation resulting in the approximation coefficients cA_1 of level 1. The latter ones are used as input for level 2, resulting again in detail coefficients cD_2 respectively in approximation coefficients cA_2 that are used for the next level etc.

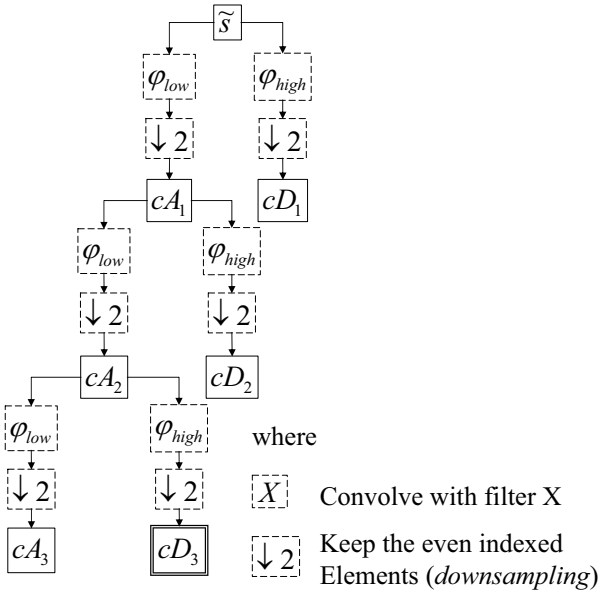

Figure 5: Principle of multilevel 1-D wavelet decomposition

The absolute degree of magnification or the interesting level of the detail coefficients respectively depends on the length of vector $\widetilde{s}_i$ and thus the level has to be adjusted according to the sampling rate – increasing or decreasing the window size does not influence the resulting frequency ranges of each level. For a sampling rate of $24kHz$, level 3 is the appropriate one and the detail coefficients cD_3 are the ones that are used in the following levels of the classifier.

For other sampling rates sr, the level can be estimated by

$$level = \lfloor (ld \frac{sr[kHz]}{3kHz} + 0,5) \rfloor \quad . \tag{6}$$

2.5 Level 2: Identifying Potential STN Signals

STN single cell activity is characteristically described as irregular or bursty. This specific behavior is used in level 2 of the classifier to decide whether a signal s_i is STN or not. Therefore, the detail coefficients cD_3 are used. We can assume that cD_3 only contains more or less only spikes of single cell activity. A single coefficient from cD_3 has a high value, if a spike with great amplitude is contained at the corresponding point in time in s_i; low values represent the absence of spikes. This result allows a straightforward algorithm: identifying those signals with variances changing over the time.

For this, each coefficient vector $cD_{3,i}$ of the corresponding signal $s_i, i \in I$ is subdivided into l_2 intervals. For each interval, the variance of coefficients is calculated. Afterwards, the difference between the smallest and largest variance of each $cD_{3,i}, i \in I$ is calculated. All the differences of the used $cD_{3,i}, i \in I$ are used to determine a threshold. Finally, a new set of indices K is created: each $s_k, k \in K$ exceeds this threshold. Therefore, the signals, the variance of which changes in time, are contained in this index set.

2.5.1 Combining Results of Level 1 and 2

From the whole set of signals, two index sets I and K are available. I represents those signals that show neuronal activity according to level 1; K contains those signals that show irregular, bursty behaviour. Furthermore, we know that $K \subset I$ holds.

At first, we concentrate on the $s_i, i \in I$. They can be partitioned in different intervals with signals $s_j, j \notin I$ in between: $s_{i_1}..s_{i_2}, s_j, s_{i_3}..s_{i_4}$ where $i_1 \leq i_2 < i_3 \leq i_4; i_1, i_2, i_3, i_4 \in I$ and $i_2 + 1 < i_3$. Those individual intervals might even contain only one recording. As the increased background activity is a major criterion for STN activity, all intervals resulting from level 1 that additionally contain at least one signal $s_k, k \in K$ are tagged as STN. For most electrodes, only one interval will fulfill this combination of criteria and this interval corresponds to the one classified as STN by the surgeon. Table 1 contains an artificial example where different combinations of the level's outcomes are shown and combined.

Index	1	2	3	4	5	6	7	8	9	10	11	12
Result 1st level	N	S	S	S	N	S	S	N	N	S	S	N
Result 2nd level	N	N	S	S	N	N	N	N	N	S	N	N
Combination	N	S	S	S	N	N	N	N	N	S	S	N

Table 1: Artificial example to illustrate the combination of results (S represents STN signals - N represents non-STN signals)

2.6 Level 3 - Removing Multiple Areas

In some rare cases, the result vector will contain multiple intervals that were classified as STN according to level 1 and 2 as shown in the example (Table 1). Typically, one interval might be STN, the other interval SNr and according to the order, the signals usually occur (see 2.1), the SNr signals will be the signals with a greater index.

To distinguish the erroneously classified signals, the spike rate or the depth can be used. The latter criterion is easy to implement: since signal acquisition is stopped as soon as SNr is reached (at the latest), the classification result of the last recordings can be revised generally.

The complexity when using the spike rate as a criterion to revise a classification is bigger. For it, the range distribution of $cd_{3,i}, i \in I$ is examined. Let $max(cd_{3,i})$ be the coefficient with the greatest value of the vector $cd_{3,i}$. Using this maximum, we define l_3 thresholds $\delta_k, 1 \leq k \leq l_3$ and calculate the values:

$$\delta_k = max(cd_{3,i}) \cdot \frac{k}{l_3} \quad . \tag{7}$$

The range of $cd_{3,i}$ can now be partitioned into l_3 equidistant intervals and we can count the number of

coefficients $\Sigma_{i,k}$ falling into each interval:

$$\Sigma_{i,k} = \sum_{delta_{k-1} < cd_{3,i} \leq delta_k} 1 \quad . \tag{8}$$

Together, the l_3 sums represent the range distribution of the corresponding coefficient vector. As some signals might contain outliers produced by the recording system, the thresholds δ_k are decreased using a linear factor until at least 10 coefficients of $cd_{3,i}$ fulfil the condition $\delta_{l_3-1} < cd_{3,i} \leq \delta_{l_3}$.

Finally, the calculated range distribution is inspected using several conditions. If the values are distributed equally on all intervals, the signal will not contain distinctive spikes and the classification of this recording can be revised. The result is also revised, if the sum of coefficients in the larger intervals is big: this recording is probably SNr.

As all signals of one interval are inspected, the classification result of the complete interval is revised if and only if at least half of the classification results of the signals belonging to this interval are revised. In Table 1, the signals s_2, s_3 and s_4 belong to one interval, signals s_{10} and s_{11} belong to another one. As already mentioned, the third level is applied if the actual classification result contains two separated intervals and thus, one of them needs to be corrected. The classification result of the second interval is revised if the result of either s_{10} or s_{11} is revised (or if both results are revised). For the first interval, a revision of the complete interval is performed if at least two of the classification results are revised.

3 Results

The MER classification system has been developed and implemented as a software prototype using Matlab^{TM}. We have used data records from Hospital of the Merciful Brethren in Trier for system development and testing. Each record contained MER data and the result of manual classification for all electrodes of one side of the head. Usually, MER acquisition begins $9mm$ in front of the image based target point and MERs are taken in $1mm$ steps. $5mm$ in front of STN, the increment is decreased to $0.5mm$. As soon as the STN is left obviously or substantia nigra (SNr) is reached, the acquisition is stopped.

From the available data and records 14 patients were selected randomly. The data included MERs of 103 electrodes and a total of 2434 recordings. A subset containing 4 left sides of 4 patients was used during system development. The remaining ones were used for validation.

Overall, 122 recordings out of 2434 were classified differently by the MER classifier as compared to surgery records. Recordings without clear assignment by the surgeon were neglected. Thus, nearly 95% of the recordings were classified correctly.

Deviations between manual and automatic classification occurred mainly in two different cases:

- One critical area is the boundary of STN, the first recordings belonging to STN and the ones when STN is left.
- Electrodes that did not show clear STN signals at all, only ambiguous signals in one or two steps, are critical too.

A few remaining deviations were due to atypical signal characteristics.

4 Discussion and Outlook

The structure of the classifier is based on a sequentially ordered means of feature extraction and according decision steps. It is built up by an hierarchical decision scheme with linear and almost univariate decision functions. Because of using a specific preprocessing and sophisticated definitions of relevant features, the feature-class relation could be considered deterministically and patient independent.

Though it could be shown, that the classifier structure is appropriate to solve the problem, some aspects of the outcome and possible enhancements can be discussed:

- classification results at the boundary of STN,
- combination of results of all levels with the aim to quantify the quality of each classification result.

The first topic contains, besides adjustments in the classifier, further analysis of the manual classification results. The relevant recordings should be presented to several experts to examine if they all agree with the classification and to learn how they decide about those recordings.

At present, the classifier produces binary decisions: STN or not-STN. With minor modifications in each level, the degree of fulfillment of a criterion can be produced in each level. E.g. not only calculating the ratio of the intervals exceeding a threshold to the amount of intervals, but also calculating the sum of differences of all intervals as a result of level 1. This would reflect the degree to which a signal is neuronal active. Analogue approaches can be developed for level 2 and 3. For example, we have introduced the extracted features into a common feature space and trained a decision system using a Fuzzy cluster algorithm. The resulting Fuzzy classifier showed at least the same results as the hierarchical one.

There exist other structures used as targets in DBS for treatment of Parkinson's disease, e.g. globus pallidus (GPi). Additionally, the treatment of other diseases like Dystonia is already common practise; other diseases like psychic illnesses are in a promising focus of research also. Therefore, the need for MER classification also occurs in other types of surgery. Extending the classifier to handle various kinds of signals seems to be a demanding but also promising field. This task is one of the problems that we are going to examine in the near future.

References

[1] J. K. Krauss, J. Jankovic, and R. G. Grossman. *Surgery for Parkinson's Disease and Movement Disorders*. Lippincott Williams and Wilkins, Philadelphia, 2001.

[2] J. K. Krauss and J. Volkmann. *Tiefe Hirnstimulation*. Steinkopff, Darmstadt, 2004.

[3] Jorge Guridi, Arancha Gorospe, Eduardo Ramos, Gurutz Linazasoro, Maria C. Rodriguez, and Jose Angel Obeso. Stereotactic targeting of the globus pallidus internus in parkinson's disease: Imaging versus electrophysiological mapping. *Neurosurgery Online*, 45(2):278–290, 1999.

[4] M. Merello, A. Cammarota, D. Cerquetti, and R. C. Leiguarda. Mismatch between electrophysiologically defined and ventriculography based theoretical targets for posteroventral pallidotomy in parkinson's disease. *Journal of Neurology, Neurosurgery and Psychiatry*, 69:787–791, 2000.

[5] J. H. Falkenberg, J. McNames, J. Favre, and K. J. Burchiel. Automatic analysis and data visualization of microelectrode recording trajectories to the subthalamic nucleus: Preliminary results. *Stereotactic and Functional Neurosurgery*, 84(1):35–45, 2006.

[6] J. McNames. Microelectrode signal analysis techniques for improved localization. In Z. Israel and K.J.Burchiel, editors, *Microelectrode Recordings in Movement Disorder Surgery*, pages 119–129, New York, 2004. Thieme.

[7] K.M.L. Menne and U.G. Hofmann. Automatic neurophysiological identification of the human subthalamic nucleus for the implantation of deep brain stimulation electrodes based on statistical signal processing methods and unsupervised classification. In *EMBEC 2005 - 3rd European Medical & Biological Engineering Conference - IFMBE European Conference on Biomedical Engineering*, pages 1727–1983, Prague, 2005. IFMBE Proceedings ISSN.

[8] Abdelhamid Benazzouz, Sorin Breit, Adnan Koudsie, Pierre Pollak, Paul Krack, and Alim-Louis Benabid. Intraoperative microrecordings of the subthalamic nucleus in parkinson's disease. *Movement disorders*, 17:145–149, 2002.

[9] W. D. Hutchison, R. J. Allan, H. OPitz, R. Levy, J. O. Dostrovsky, A. E. Lang, and A. M. Lozano. Neurophysiological identification of the subthalamic nuclues in surgery for parkinson disease. *Annals of Neurology*, 44(4):622–628, 1998.

[10] David L. Donoho. De-noising by soft-thresholding. *IEEE Transactions on Information Theory*, 41(3):613–627, 1995.

[11] Ingrid Daubechies. *Ten lectures on wavelets*. Society for Industrial and Applied Mathematics, 1992.

[12] Werner Bäni. *Wavelets*. Oldenbourg, München, Germany, 2002.